Icarus 229 (2014) 278–294

Contents lists available at ScienceDirect

Icarus

journal homepage: www.elsevier.com/locate/icarus

Stability of rubble-pile satellites

Ishan Sharma *

Department of Mechanical Engineering, IIT Kanpur, Kanpur 208016, India
Mechanics & Applied Mathematics Group, IIT Kanpur, Kanpur 208016, India

ARTICLE INFO

Article history:
Received 19 April 2013
Revised 21 September 2013
Accepted 24 September 2013
Available online 26 October 2013

Keywords:
Satellites, dynamics
Satellites, composition
Satellites, shapes
Geophysics
Interiors

ABSTRACT

We consider the stability of rubble-pile satellites that are held together by their own gravity. A satellite is said to be stable whenever it is both orbitally and structurally stable to both orbital and structural perturbations. We restrict attention to satellites whose dimensions are small compared to their respective orbital radii and their associated planets' sizes. In this case, we show that a satellite is stable whenever it is orbitally stable to orbital perturbations and structurally stable to structural perturbations. Orbital stability is investigated by a spectral analysis, while structural stability is probed by appropriately extending the work of Sharma [Sharma, I., 2012. Stability of rotating non-smooth complex fluids. J. Fluid Mech. 708, 71–99; Sharma, I., 2013. Structural stability of rubble-pile asteroids. Icarus 223, 367–382]. The stability test is then applied to planetary satellites of the Solar System that are suspected to be granular aggregates, including many of the recently discovered smaller moons of the giant planets.

1. Introduction

Many planetary satellites including those of Mars and some of the newly discovered moons of the giant planets are suspected to be granular aggregates held together by self gravity alone. The equilibrium shapes of these objects have been previously analyzed utilizing volume-averaging by Sharma (2009), henceforth Paper I, assuming them to be of ellipsoidal shape and on tidally-locked circular orbits about a massive, possibly oblate, central planet. In the context of shapes and failure of solid satellites, we also mention related work of Aggarwal and Oberbeck (1974) who estimated the Roche limit of an elastic and spherical satellite while assuming brittle failure, Dobrovolskis (1990) who combined the Navier criterion for failure of sandy materials with an elastic stress analysis of ellipsoids, Davidsson (1999, 2001) who assumed that the satellite failed when the maximum value of the average normal stress across some critical plane within the satellite surpassed the constituent material's tensile strength, and Holsapple and Michel (2006, 2008) who employed limit analysis and a pressure-dependent Mohr–Coulomb yield condition to investigate the equilibrium of granular ellipsoids in the presence of self-gravity and tidal interaction. The equilibrium shapes of fluid satellites has, of course, been extensively studied, see, e.g., Chandrasekhar (1969, Chapter 8).

Stability analyses of planetary satellites has typically focussed on the orbital stability of these objects, disregarding the response of the satellite as a distributed mass that may possibly yield and deform significantly. In astrophysical applications, structural stability of orbiting fluid ellipsoids has, however, been investigated. These fall under the stability of Roche and Darwin ellipsoids; see Chandrasekhar (1969, Chapter 8). Some recent advances are due to Lai et al. (1993) who considered the stability of compressible inviscid fluid Roche and Roche-Riemann ellipsoids. These authors tested stability by minimizing an energy functional that was allowed to depend on parameters such as the ellipsoid's shape, density, mass, angular momentum, and internal vorticity.

Here, we investigate the stability of granular satellites. A satellite will be deemed stable only if its orbit and its structure are both stable to both orbital and structural perturbations. Here, by structure we mean the collection of material points that constitute the satellite, and structural stability refers to this collective staying close to its equilibrium configuration; we will discuss stability more precisely in Section 5. In the case of satellites whose primaries are much more massive, we will show in Section 5.2 that orbital and structural stability may be considered separately. While orbital stability may then be determined by standard methods, structural stability will be gauged by suitably extending Sharma's (2013) stability analysis of asteroids to the case of satellites by including the effect of tidal forces. We limit ourselves to homogeneous velocity perturbations of the equilibrium state. For definiteness, at equilibrium the satellite will be assumed to be of ellipsoidal shape and on a circular orbit about a massive primary; see Fig. 1. While the present framework may be utilized for the stability analysis of any satellite system wherein the primary is much larger than the secondary, we will present final calculations suitable for spheroidal primaries and will be most suitable for planetary satellites. Other shapes of the primary may be probed

* Address: Department of Mechanical Engineering, IIT Kanpur, Kanpur 208016, India.
E-mail address: ishans@iitk.ac.in

0019-1035/$ - see front matter
http://dx.doi.org/10.1016/j.icarus.2013.09.023

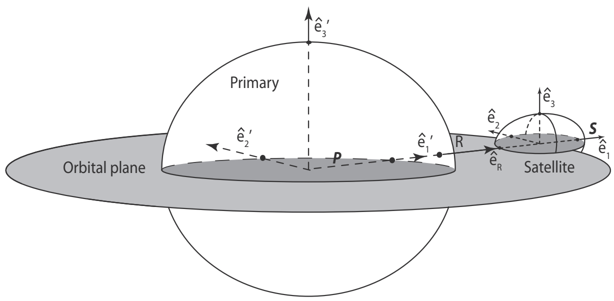

Fig. 1. Equilibrium configuration of an ellipsoidal satellite of an oblate planet. The unit vector $\hat{e}_R$ locates the satellite with respect to the planet's center.

by appropriately modifying the tidal shape tensor, and this would extend the applicability of the current analysis to asteroidal satellites.

We first derive the equations for a homogeneously deforming ellipsoidal satellite.

2. Satellite dynamics

2.1. Structural deformation

Paper I derives equations for a homogeneously deforming ellipsoidal satellite of an oblate planet. For such a body, a material point's velocity is linearly dependent on its location with respect to the ellipsoid's center. In stability investigations, it is expedient to phrase these equations in a frame $\mathcal{O}$ rotating at $\boldsymbol{\omega}(t)$ and attached to the satellite's centroid S. With $\boldsymbol{\omega}(t)$ we associate an anti-symmetric *angular-velocity tensor* $\boldsymbol{\Omega}(t)$ satisfying

$$\boldsymbol{\omega} \times \mathrm{x} = \boldsymbol{\Omega} \cdot \mathrm{x}, \tag{1}$$

where x is a material point's location relative to S; $\boldsymbol{\omega}$ is $\boldsymbol{\Omega}$'s associated *axial vector*. We employ such rotation rate vectors and their corresponding tensors interchangeably.

In the rotating frame $\mathcal{O}$, for a homogeneously deforming ellipsoid, a material point's velocity relative to the ellipsoid's center is

$$\dot{\mathrm{x}} = \boldsymbol{L} \cdot \mathrm{x}, \tag{2}$$

where the dot $(\dot{\cdot})$ indicates time derivative with respect to an observer in $\mathcal{O}$ and $\boldsymbol{L}$ is the *velocity gradient* observed in $\mathcal{O}$ that depends only on time. The tensor $\boldsymbol{L}$ estimates the local rate of change of relative displacement, while its symmetric ($\boldsymbol{D}$) and anti-symmetric ($\boldsymbol{W}$) parts capture local deformation and rotation rates, respectively. The governing equations for homogeneous dynamics as observed in $\mathcal{O}$ were found by Sharma (2013) to be

$$(\dot{\boldsymbol{L}} + \boldsymbol{L}^2) \cdot \boldsymbol{I} = -\overline{\boldsymbol{\sigma}} V + \boldsymbol{M}^T - (\dot{\boldsymbol{\Omega}} + \boldsymbol{\Omega}^2 + 2\boldsymbol{\Omega} \cdot \boldsymbol{L}) \cdot \boldsymbol{I} \tag{3a}$$

$$\text{and} \quad \dot{\boldsymbol{I}} = \boldsymbol{L} \cdot \boldsymbol{I} + \boldsymbol{I} \cdot \boldsymbol{L}^T, \tag{3b}$$

where $\overline{\boldsymbol{\sigma}}$ is the volume-averaged stress tensor,

$$\boldsymbol{I} = \int_V \rho \mathrm{x} \otimes \mathrm{x}\, dV \tag{4a}$$

$$\text{and} \quad \boldsymbol{M} = \int_V \rho \mathrm{x} \otimes \mathrm{b}\, dV, \tag{4b}$$

are, respectively, the ellipsoid's inertia tensor and external moment tensor due to applied body forces b, and ρ and V are the ellipsoid's density and volume, respectively. In (3a), the last three bracketed terms on the right-hand side are, respectively, angular, centripetal and Coriolis' accelerations, and act as external moment tensors in the rotating frame $\mathcal{O}$. Equation (3a) follows $\boldsymbol{L}$'s evolution in $\mathcal{O}$ by balancing internal stresses, external moments and inertial effects, while (3b) describes the changing inertia tensor. We note that $\boldsymbol{I}$ is different from the Euler moment of inertia tensor $\boldsymbol{J}$ commonly employed in rigid body mechanics; cf. (25).

The tensor $\boldsymbol{M}$ includes the effect of the satellite's own gravity and that of the planet. The moment due to the satellite's self-gravity is found by Sharma et al. (2009) to be

$$\boldsymbol{M}_G = -2\pi\rho G \boldsymbol{I} \cdot \boldsymbol{A}, \tag{5}$$

where $\boldsymbol{A}$ is the *gravitational shape tensor* that captures the effect of the satellite's ellipsoidal shape on its internal gravity. The tensor $\boldsymbol{A}$ is diagonalized in the satellite's principal axes coordinate system, and its components in that frame are available in Sharma et al. (2009). The gravitational force exerted on a unit mass within the satellite at $\mathrm{X} = \mathrm{x} + R\hat{e}_R$ by an ellipsoidal planet is

$$\mathrm{b}_Q = -2\pi\rho' G \boldsymbol{B} \cdot \mathrm{X}, \tag{6}$$

where ρ' is the planet's density and $\boldsymbol{B}$ is the *tidal shape tensor* that captures the effect of the planet's ellipsoidal shape and depends on X and the planet's semi-major axes a'_i. The tensor $\boldsymbol{B}$ is diagonalized in the planet's principal axes frame and depends on the *ellipsoidal coordinate* of the material point at X; see Eq. (19) of Paper I. To estimate the tidal moment, we first expand $\boldsymbol{B}$ as

$$\boldsymbol{B} = \boldsymbol{B}^{(0)} + \boldsymbol{\mathcal{B}}^{(1)} \cdot \frac{\mathrm{x}}{R} + \mathbb{B}^{(2)} : \frac{\mathrm{x} \otimes \mathrm{x}}{R^2} + \cdots,$$

where $\boldsymbol{B}^{(0)}, \boldsymbol{\mathcal{B}}^{(1)}$ and $\mathbb{B}^{(2)}$ are, respectively, second-, third- and fourth-order tensors, and, in indical notation, $(\boldsymbol{\mathcal{B}}^{(1)} \cdot \mathrm{x})_{ij} = B^{(1)}_{ijk} x_k$ and $(\mathbb{B}^{(2)} : \mathrm{x} \otimes \mathrm{x})_{ij} = B^{(2)}_{ijkl} x_l x_k$. Note that because $\boldsymbol{B}$ is a symmetric tensor, so too is $\boldsymbol{B}^{(0)}$, while $\boldsymbol{\mathcal{B}}^{(1)}$ and $\mathbb{B}^{(2)}$ are symmetric in their first two arguments, i.e., $B^{(1)}_{ijk} = B^{(1)}_{jik}$ and $B^{(2)}_{ijkl} = B^{(2)}_{jikl}$. We then substitute the above expansion in (4b) and compute the resulting integrals, to obtain the tidal moment due to the planet correct up to $O(|\mathrm{x}|^3/R^3)$ as

$$\boldsymbol{M}_Q = -2\pi\rho' G \boldsymbol{I} \cdot \left[\boldsymbol{B}^{(0)} + \left(\hat{e}_R \cdot \boldsymbol{\mathcal{B}}^{(1)}\right)^T\right], \tag{7}$$

where $\left(\hat{e}_R \cdot \boldsymbol{\mathcal{B}}^{(1)}\right)_{jk} = e_{R_i} B^{(1)}_{ijk}$; see Paper I for more details. The total moment is then

$$\boldsymbol{M} = \boldsymbol{M}_G + \boldsymbol{M}_Q = -2\pi\rho G \boldsymbol{I} \cdot \boldsymbol{A} - 2\pi\rho' G \boldsymbol{I} \cdot \left[\boldsymbol{B}^{(0)} + \left(\hat{e}_R \cdot \boldsymbol{\mathcal{B}}^{(1)}\right)^T\right]. \tag{8}$$

Equation (3) along with (8) follow a homogeneously deforming ellipsoidal satellite's structural motion relative to frame $\mathcal{O}$.

We now describe the satellite's orbital motion about the planet.

2.2. Orbital motion

To track the satellite's orbit, we equate the total force F acting on the satellite to its mass center's acceleration:

$$m\{\ddot{\mathrm{R}} + (\dot{\boldsymbol{\Omega}} + \boldsymbol{\Omega}^2) \cdot \mathrm{R} + 2\boldsymbol{\Omega} \cdot \dot{\mathrm{R}}\} = \mathrm{F}, \tag{9}$$

where m is the satellite's mass and the left-hand side is the absolute acceleration of the satellite's mass center written in the rotating frame $\mathcal{O}$. The total force F exerted by the oblate planet on the satellite is obtained by computing $\int \rho \mathrm{b}_Q\, dV$ with b_Q given by (6). Employing $\boldsymbol{B}$'s expansion from Section 2.1 of Paper I finds

$$\mathrm{F} = -2\pi\rho' G R m \left[\boldsymbol{B}^{(0)} \cdot \hat{e}_R + \frac{1}{mR^2}\left(\boldsymbol{\mathcal{B}}^{(1)} + \hat{e}_R \cdot \mathbb{B}^{(2)}\right) : \boldsymbol{I}\right],$$

correct up to $O(|\mathrm{x}|^3/R^3)$ and $\left\{\left(\boldsymbol{\mathcal{B}}^{(1)} + \hat{e}_R \cdot \mathbb{B}^{(2)}\right) : \boldsymbol{I}\right\}_j = \left(B^{(1)}_{jkl} + \hat{e}_{R_i} B^{(2)}_{ijkl}\right) I_{kl}$. Because $\boldsymbol{I}/mR^2$ scales as $\bar{a}^2/R^2$, where $\bar{a}$ is the satellite's average diameter, we may, for satellite systems where the separation from the planet is much greater than the satellite's size, approximate F as

$$\mathrm{F} \approx -2\pi\rho' G m \boldsymbol{B}^{(0)} \cdot \mathrm{R}. \tag{10}$$